RSC Advances

Cite this: *RSC Advances*, 2012, **2**, 6729–6732

www.rsc.org/advances

COMMUNICATION

Thermally responsive microlens arrays fabricated with the use of defect arrays in a smectic liquid crystal†

Jung Hyun Kim,[a] Yun Ho Kim,[b] Hyeon Su Jeong,[c] Mohan Srinivasarao,[d] Steve D. Hudson[e] and Hee-Tae Jung*[a]

Received 27th March 2012, Accepted 4th June 2012
DOI: 10.1039/c2ra20561k

Defects in a smectic liquid crystal, toric focal conic domains (TFCDs), were developed for the fabrication of thermally responsive microlens arrays. In this system, each TFCD acts as a separate focusing unit *via* the intrinsic molecular orientation of the TFCDs, and the focusing ability of the microlens varies with local environmental temperature.

With advances in miniaturization, microlens systems have been of considerable interest in photonic waveguides, electronic displays and miniature optical sensing devices.[1–3] Among the microlens systems in particular, a dynamically adjustable microlens that is field responsive has attracted a great deal of attention in recent years because of its attractive abilities, such as extinction for optical switching applications and field of view change for multiple imaging.[4–6] A number of attempts, which included electrowetting of liquid droplets,[5,7–9] re-orientation of liquid crystals (LCs)[10,11] and mechanical actuation of polymeric materials[12–15] and responsive hydrogels,[16,17] have been fabricated that are dynamic in nature, with good focal length tunability. However, these approaches are not without their shortcomings, as they involve multiple fabrication steps requiring expensive equipment. For example, previous LC microlenses in the presence of an external electric field required a complex LC cell structure in combination with circular hole-patterned electrodes and polymer stabilizers.[6,18] Furthermore, all previous systems have adopted conventional spherical or hemispherical shapes with a homogenous refractive index to fabricate microlenses.

Recently, we have reported the optical characteristics of the toric focal conic domains (TFCDs), which were all made of unique smectic LC material with a semi-fluorinated chain.[19,20] However, TFCD based microlens arrays (MLAs) using a semi-fluorinated LC have difficulty in having thermally tunable properties. First of all, the semi-fluorinated LC molecules are very easily sublimated above the smectic A phase region (<114 °C) (Fig. S1†). In order to avoid sublimation problems, therefore, MLAs made by the semi-fluorinated LC should be operated in the soft crystal phase. In the soft crystal phase, however, MLAs using the semi-fluorinated LC could not have good lens properties, because each TFCD structure distorted and cracked slightly through the soft crystal phase.

Here, we show what we believe to be a new approach to fabricate thermally responsive MLAs using a commercial LC, **8CB** (4′-n-octyl-4-cyano-biphenyl), which forms a smectic phase on cooling from the isotropic melt through the nematic phase. The microlens characteristics appear in the ordered TFCDs that are generated in the smectic phase of **8CB** molecules confined within surface modified trapezoidal channels.[21] This system focuses light using the intrinsic LC molecular orientations in TFCDs rather than geometrical shape, and shows microlens performance.[19,22,23] The microlens effect disappears in the isotropic and the nematic phases due to variation of the molecular orientation, and appears again in the smectic phase. Thus, the thermally responsive microlens system can be created rather easily by just changing the temperature. This system has remarkable advantages over previous thermally reversible MLAs, in that it has a fast response to temperature changes, due to high mobility of the **8CB** molecules, and is easy to prepare because of the low smectic–nematic phase transition temperature (32.2 °C). Furthermore, the focal length and array number of the microlenses can be easily controlled by varying the feature dimensions of the confining channel. Thus, this provides a facile fabrication of the thermally responsive MLAs with a variety of focal lengths (which are tunable), with the number of lenses being easily controllable by the periodic defect structure.

Fig. 1 illustrates the overall scheme for fabricating the ordered TFCDs in a trapezoid-shaped micro-channel. We used a commercially available liquid crystal, **8CB** (Fig. 1a), which possesses a smectic to nematic transition (32.2 °C) upon cooling from the isotropic melt. To fabricate periodic TFCD arrays of **8CB**, we selected polyethyleneimine (PEI, ~10 nm thick) coated trapezoidal microchannels (Fig. 1b and 1c). The shape and surface of the channel are essential for fabrication of thermally-responsive MLAs using a thermotropic **8CB** liquid crystal. The V-shaped and rectangular-shaped channels did not form such regular TFCDs.[21,24] It was found that the channel must be coated with PEI in order for the TFCD array to form reliably. **8CB** was filled into the PEI-coated trapezoidal channels by capillary force in its isotropic phase. It should be noted

[a]*Department of Chemical and Biomolecular Engineering, Korea Advanced Institute of Science and Technology, Daejeon, 305-701, Korea. E-mail: heetae@kaist.ac.kr; Fax: +82-42-350-3910; Tel: +82-42-350-3931*
[b]*Advanced Functional Materials Research Group, Korea Research Institute of Chemical Technology, Daejeon 305-600, Korea*
[c]*Optical Materials Lab, SK innovation, Daejeon, 205-712, Korea*
[d]*School of Materials Science and Engineering, School of Chemistry and Biochemistry, Georgia Institute of Technology, Atlanta, GA 30022, USA*
[e]*Polymer Division, National Institute of Standards and Technology, Gaithersburg, Maryland, 20899, USA*

† Electronic Supplementary Information (ESI) available: TGA data of the smectic LC compound with sublimation problems (S1), SEM images of the template (S2), OM images of MLAs at z = 0, z = focal length (S3), temperature available range of this MLA system (S4). See DOI: 10.1039/c2ra20561k

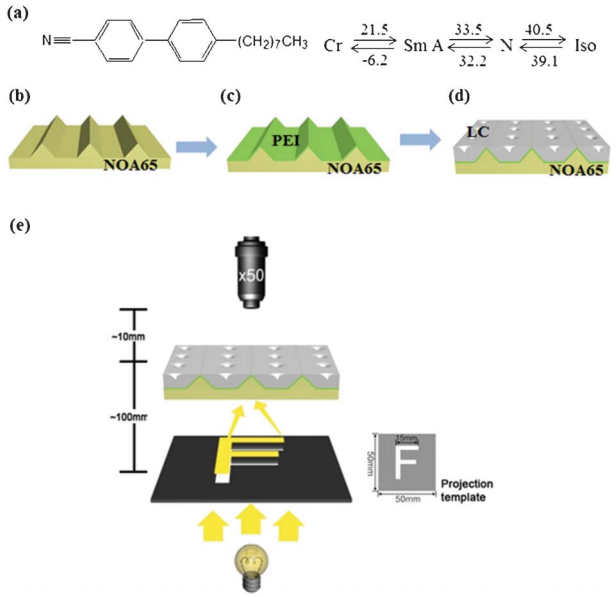

Fig. 1 (a) The molecular structure and the phase transition temperatures of the smectic LC compound. (b–d) A schematic representation of the LC MLAs. (e) The experimental setup for the projection experiment. MLA samples were scanned in the z-direction of the microscope to determine the focal planes of the MLAs. A black polymer sheet with a transparent letter "F" was prepared by a laser printer (HP Laser Jet-2420).

that the thickness of the LC film can be precisely controlled, simply by varying the depth of the microchannel. Upon cooling (-1 °C min^{-1}) from the isotropic to the smectic phase, ordered TFCD arrays formed in the PEI-coated trapezoidal channel (Fig. 1d). Fig. 1e represents an experimental setup of the projection experiment using the LC based MLAs. The MLAs were positioned on the sample stage of an optical microscope (Nikon, LV100-Pol). A transparent letter "F" (size: 15 mm × 15 mm) on a black sheet was placed under the MLAs.[25] We used a UV-curable polymer NOA65 (Norland Optical Adhesives 65) composite, made from an acrylate monomer and a mercapto-ester, to fabricate the trapezoidal channels. Because the trapezoid-shaped NOA65 channel substrates are highly transparent in the visible spectrum,[26] the light passing through this template was projected through the TFCD arrays. The resulting projected images were observed through the objective lens of a light microscope. The sample was scanned in the z-direction of the microscope to determine the focal plane of each MLA.

Fig. 2 shows optical microscopy (OM) and polarized optical microscopy (POM) images and their corresponding schematic models of three different phases of **8CB** in the PEI-coated trapezoidal channels: the isotropic phase (Fig. 2a–c), the nematic phase (Fig. 2d–f) and the smectic phase (Fig. 2g–i). In the isotropic phase, the cell appears dark under crossed polarizers (Fig. 2b), thus indicating that the LC molecules are randomly oriented without any long range order (Fig. 2c). In the nematic phase, the POM image exhibits two or four point defects in the channel. This corresponds to director singularities (Fig. 2d) in the Schlieren texture, which is a typical texture in the nematic liquid crystalline phase (Fig. 2e). Since the hydrophilic cyano-group (C≡N) in the **8CB** molecule prefers a planar orientation at the **8CB**–PEI interface, but the **8CB** molecules prefer a homeotropic orientation at the LC–air interface, the LC molecules have a tangential alignment at the bottom and side walls

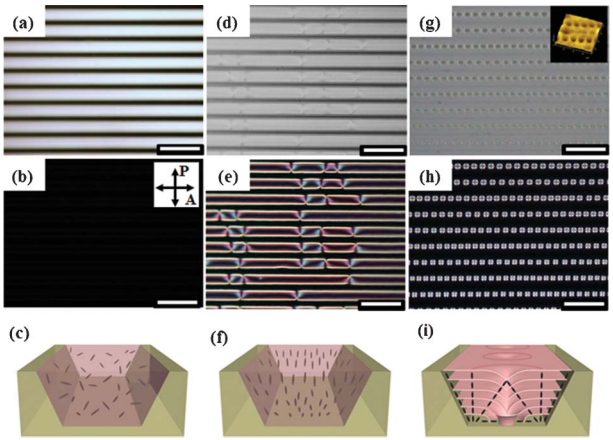

Fig. 2 OM and POM images, and a schematic representation of **8CB** at different temperatures in trapezoidal microchannels with the upper side, lower side and depth of the channel, u = 20 μm, l = 8.2 μm and h = 8.3 μm (scale: 50 μm). (a–c) At 42 °C (isotropic phase region), (d–f) at 35 °C (nematic phase region), (g–i) at 32 °C (smectic phase region). Inset (g): atomic force microscopy (AFM) three-dimensional topography of linear TFCD arrays at the LC–air interface of the channel. In (c), (f) and (i), the gray rods represent each LC molecule.

of the channel and a perpendicular alignment to the substrate at the LC–air surfaces (Fig. 2f). Upon cooling to the smectic phase, a perfect ordering of toroidal objects forms over the entire channel length (10 mm long) in the PEI-modified trapezoidal channel (Fig. 2g). These domains are TFCDs, which are formed by bending smectic layers to satisfy the antagonistic anchoring condition. A detailed examination of the surface topology of the specimen by atomic force microscopy (AFM) confirmed that these toroidal patterns are associated with corresponding depressions of the SmA–air interface, which resulted from bending the SmA layers around the axial defect core of the TFCD (Fig. 2g, inset).[27,28] Each TFCD creates a characteristic Maltese cross pattern, which indicates that the smectic director (surface normal of the layers) on the plane of the substrate is radial within the circle area. Outside the circular base, the molecules are homeotropically aligned with respect to the bottom substrate, thus these areas are observed to be dark under crossed polarizers (Fig. 2h). Fig. 2i shows the schematic illustration of TFCDs in the trapezoidal channel. The molecules are aligned tangentially at the bottom and at the inclined side walls, while they are aligned perpendicularly to the free surface. These anchoring preferences are ultimately responsible for the formation of TFCD arrays. The layer curvatures are accommodated by two defect lines: a straight line perpendicular to the plane of the substrate, which serves as the axis of rotational symmetry of the TFCD; and a circular line at the bottom of the channel. We note that each TFCD structure can act as a microlens due to the intrinsic molecular orientation of the TFCD. At the z = 0 position, where the focal point of the objective lens was located at the top surface of the MLA substrate, a non-diffracted image of the MLA was captured. However, when the focal point of the objective lens was adjusted upwards to match the focal plane of the MLAs, the letter "F" was clearly observed (Fig. S3†).

Therefore, **8CB** molecules in the PEI-modified trapezoidal channel are capable of fabricating thermally responsive MLAs, which use the phase transition of the thermotropic **8CB** liquid crystal. Fig. 3 shows a series of OM images at each temperature during cooling

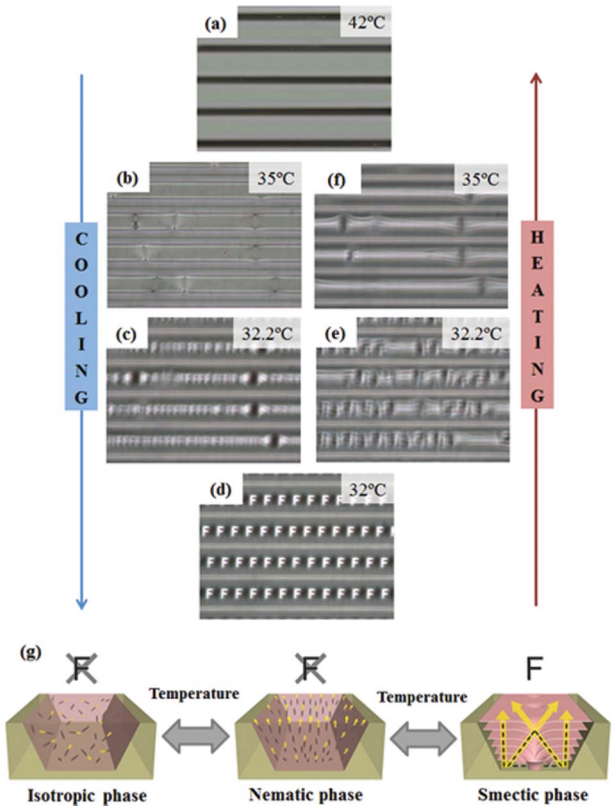

Fig. 3 Series of OM images taken during the cooling (Fig. 3a–d) and heating (Fig. 3d–f) processes between the isotropic phase (42 °C) and the smectic phase (32 °C). The cooling and heating rate are 1 °C min^{-1}. (g) Mechanism for the thermal response of the TFCD MLAs.

(Fig. 3a–d) and heating (Fig. 3e,f) at a rate of 1 °C min^{-1}. No diffracted images of the MLA were observed until the temperature reached the nematic–smectic phase transition temperature ($T_{N–SmA}$ = 32.2 °C) (Fig. 3a and 3b). When the temperature reaches the $T_{N–SmA}$, the letter 'F' gradually appears (Fig. 3c), and on further cooling into the smectic phase, the image is well defined, as illustrated in Fig. 3d. Thus, this is evidence that a TFCD can function as a microlens due to its intrinsic molecular structure. As the temperature was decreased to room temperature, the structure was retained indefinitely, for as long as the sample was in the smectic phase. When the temperature rose to $T_{N–SmA}$, the MLA gradually disappeared (Fig. 3e and 3f) due to the phase changes with temperature. It is noteworthy that it took only a few seconds (about 4 s) to generate uniform TFCD arrays over the entire microchannel, due to the high mobility of the **8CB** molecules. On further cooling through the melting point (−6.2 °C), the material crystallized, thus leading to the destruction of structure that is responsible for the MLAs (Fig. S4†). Fig. 3g shows a possible mechanism for the switching ability of the LC based MLA arrays in the different fluid phases. At temperatures above the clearing point of **8CB**, the molecules are randomly oriented and hence do not possess the molecular alignment necessary for focusing a light beam. The MLA features would not be changed in the nematic phase, because the Schlieren texture of the nematic phase does not have any focusing units for the light. Upon cooling (−1 °C min^{-1}) to the smectic phase, however, ordered TFCD arrays are formed, and each TFCD structure can be a focusing unit. The effective refractive index of the TFCD varies gradually according to the intrinsic molecular orientations in a TFCD. Because of the dimple structure of TFCDs, which bends the smectic layers toward the center of the domain, the local effective refractive index increases at the center region of the TFCD. As the incident light is passing through a TFCD, the light is refracted according to the **8CB** molecule and focused on the center of the TFCD. Therefore, each TFCD can act as a gradient index microlens. As the phase transition of the LC is reversible, TFCD arrays can be thermally responsive MLAs.

We found that the array number and focal length of the microlenses could be easily controlled by varying the feature dimensions of the confined trapezoidal channel, which were defined by the upper side (u), lower side (l) and depth (h). In our previous work, we found that the size and ordering of TFCD arrays can be strongly affected by the feature dimensions, especially l and h of the trapezoidal channel.[21] We used trapezoidal channels with five different dimensions (table in Fig. 4): the depth was fixed at h = 8.3 μm for the isosceles trapezoidal forms. Fig. 4a–4e show optical micrograph images projected through MLAs with various sizes and numbers. In all channels, miniaturized "F" images were clearly visible. In Fig. 4a–4e, the size of the channels was enlarged; u = 20–50.5 μm and l = 8.2–38.7 μm with fixed h = 8.3 μm. The size of the TFCDs was measured by the center-to-center distance at the z = 0 position. The average diameter $<2a>$ of the TFCDs increased with channel width (table in Fig. 4).[29] Furthermore, multiple-row arrays of TFCDs form, in which the equilibrium diameter of the TFCDs is smaller than the width of the channels. Fig. 4c–4e show the arrangement of microlenses on 8.3 μm deep trapezoidal channels with increasing u = 31.2–50.5 μm and l = 19.4–38.7 μm. The diameter of the microlenses increased from the formation of a single-row array to a 2-row and 3-row array. Moreover, the focal length of the MLAs that produced the clearest images of the letter "F" increased almost linearly with TFCD size (Fig. 4f).

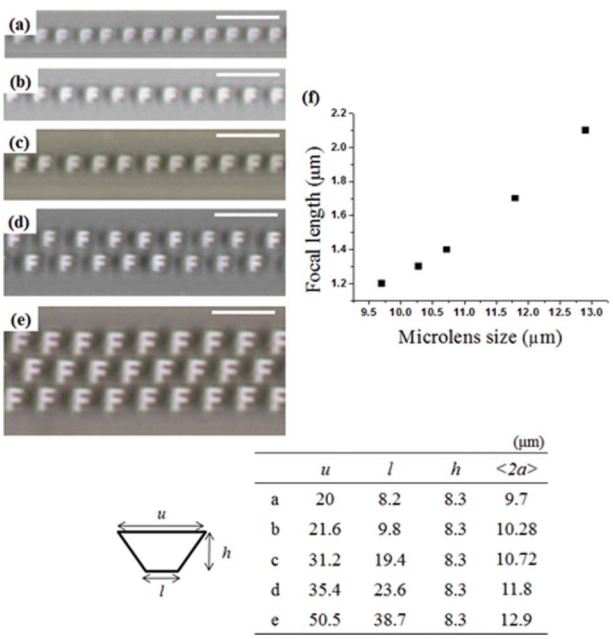

(μm)

	u	l	h	$<2a>$
a	20	8.2	8.3	9.7
b	21.6	9.8	8.3	10.28
c	31.2	19.4	8.3	10.72
d	35.4	23.6	8.3	11.8
e	50.5	38.7	8.3	12.9

Fig. 4 (a–e) OM images projected through MLAs with various numbers. Detailed information on the trapezoidal channels is shown in the table. All scale bars indicate 25 μm. (f) Focal length as a function of size of the TFCD microlens. The focal length increased almost linearly with TFCD size.

Experimental

Sample preparation

V-shaped microchannels were fabricated on (100) Si wafers using photolithography, in which the features of the channels were controlled by precisely tuning the wet etching conditions. Trapezoidal channels are fabricated by replica molding with a V-shaped microchannel using Norland Optical Adhesive 65 (NOA65). NOA65, a UV curable polymer, was poured onto the V-shaped microchannel and immediately irradiated for 8 h with UV light (350 nm) at ambient temperature. The source of UV light was a Xenon arc lamp operating at 200 W electrical power. The NOA65 replica molds we fabricated were trapezoidal and 20–50.5 μm wide, 7.3–8.3 μm deep and 10 mm long. To prepare a substrate with planar anchoring of the LC, polyethyleneimine (PEI) was spin-coated on a NOA65 replica mold after air plasma treatment. **8CB** was placed on the microchannel and then heated to the isotropic temperature of the LC in order to be injected into the channel by capillary force. The channel was filled with the LC completely; hence the thickness of the SmA film was approximately equal to the depth of the channel. Then, the sample was cooled to the SmA phase (from 40.5 °C to 33.5 °C) at a rate of 1 °C min^{-1}. To observe the temperature limit of the system, the sample was cooled at a temperature below the crystal to SmA transition by purging with liquid nitrogen.

Characterization

Textures of SmA were observed by polarizing optical microscopy (POM) (LV-100POL, Nikon) equipped with a temperature controlled stage, attached to a liquid nitrogen pump and a charge-coupled device (CCD) camera.

Conclusions

In summary, we have demonstrated a simple and facile method for fabricating thermally responsive MLAs using thermotropic liquid crystals that exhibit a smectic A phase. Each TFCD could act as a microlens because of the intrinsic structure of TFCDs, and it can be reversibly controlled by temperature because of its ability to achieve fast stabilization of molecular ordering and structure, due to the reversible and noncovalent interactions of the LC molecules. Also, the size, focal length and number of MLAs could easily be controlled by simply changing the confined dimensions of the trapezoidal channels. MLAs with a fast thermal response can be a powerful tool for realizing their applications in temperature sensitive sensors and optical devices.

Acknowledgements

This work was supported by the Korea Research Foundation Grant (KRF-2009-013-D00033).

References

1 R. Sawada, J. Shimada, E. Higurashi and T. Ito, *J. Micromech. Microeng.*, 1999, **9**, 71–77.
2 T. N. Oder, J. Shakya, J. Y. Lin and H. X. Jiang, *Appl. Phys. Lett.*, 2003, **82**, 3692–3694.
3 G. Lee, B. Yoon, H. Acharya, C. Park and J. Huh, *Macromol. Res.*, 2009, **17**, 181–186.
4 E. C. Tam, *Opt. Lett.*, 1992, **17**, 369–371.
5 S. Kuiper and B. H. W. Hendriks, *Appl. Phys. Lett.*, 2004, **85**, 1128–1130.
6 H. W. Ren, D. Fox, P. A. Anderson, B. Wu and S. T. Wu, *Opt. Express*, 2006, **14**, 8031–8036.
7 S. Yang, T. N. Krupenkin, P. Mach and E. A. Chandross, *Adv. Mater.*, 2003, **15**, 940.
8 M. A. Bucaro, P. R. Kolodner, J. A. Taylor, A. Sidorenko, J. Aizenberg and T. N. Krupenkin, *Langmuir*, 2009, **25**, 3876–3879.
9 M. Im, D. H. Kim, J. H. Lee, J. B. Yoon and Y. K. Choi, *Langmuir*, 2010, **26**, 12443–12447.
10 T. Kyu and D. Nwabunma, *Macromolecules*, 2001, **34**, 9168–9172.
11 Y. Choi, J. H. Park, J. H. Kim and S. D. Lee, *Opt. Mater.*, 2003, **21**, 643–646.
12 N. Chronis, G. L. Liu, K. H. Jeong and L. P. Lee, *Opt. Express*, 2003, **11**, 2370–2378.
13 D. Y. Zhang, V. Lien, Y. Berdichevsky, J. Choi and Y. H. Lo, *Appl. Phys. Lett.*, 2003, **82**, 3171–3172.
14 B. H. Hu, L. J. Xue, P. Yang and Y. C. Han, *Langmuir*, 2010, **26**, 6350–6356.
15 J. Perera-Nunez, A. Mendez-Vilas, L. Labajos-Broncano and M. L. Gonzalez-Martin, *Langmuir*, 2010, **26**, 17712–17719.
16 L. Dong, A. K. Agarwal, D. J. Beebe and H. Jiang, *Adv. Mater.*, 2007, **19**, 401–405.
17 A. M. Trunfio-Sfarghiu, Y. Berthier, M. H. Meurisse and J. P. Rieu, *Langmuir*, 2008, **24**, 8765–8771.
18 S. Masuda, S. Takahashi, T. Nose, S. Sato and H. Ito, *Appl. Opt.*, 1997, **36**, 4772–4778.
19 Y. H. Kim, H. S. Jeong, J. H. Kim, E. K. Yoon, D. K. Yoon and H. T. Jung, *J. Mater. Chem.*, 2010, **20**, 6557–6561.
20 Y. H. Kim, J. O. Lee, H. S. Jeong, J. H. Kim, E. K. Yoon, D. K. Yoon, J. B. Yoon and H. T. Jung, *Adv. Mater.*, 2010, **22**, 2416–2420.
21 J. H. Kim, Y. H. Kim, H. S. Jeong, E. K. Yoon and H. T. Jung, *J. Mater. Chem.*, 2011, **21**, 18381–18385.
22 Y. H. Kim, D. K. Yoon and H. T. Jung, *J. Mater. Chem.*, 2009, **19**, 9091–9102.
23 Y. H. Kim, D. K. Yoon, H. S. Jeong, O. D. Lavrentovich and H. T. Jung, *Adv. Funct. Mater.*, 2011, **21**, 610–627.
24 M. C. Choi, T. Pfohl, Z. Y. Wen, Y. L. Li, M. W. Kim, J. N. Israelachvili and C. R. Safinya, *Proc. Natl. Acad. Sci. U. S. A.*, 2004, **101**, 17340–17344.
25 H. Yabu and M. Shimomura, *Langmuir*, 2005, **21**, 1709–1711.
26 B. P. Iguanero, A. O. Perez and I. F. Tapia, *Opt. Mater.*, 2002, **20**, 225–232.
27 V. Designolle, S. Herminghaus, T. Pfohl and C. Bahr, *Langmuir*, 2006, **22**, 363–368.
28 W. Guo, S. Herminghaus and C. Bahr, *Langmuir*, 2008, **24**, 8174–8180.
29 Y. H. Kim, D. K. Yoon, M. C. Choi, H. S. Jeon, M. W. Kim, O. D. Lavrentovich and H. T. Jung, *Langmuir*, 2009, **25**, 1685–1691.